

# Compression of Medical Images using Wavelet Transforms

Ruchika, Mooninder Singh, Anant Raj Singh

**Abstract**— Medical image compression is necessary for huge database storage in Medical Centres and medical data transfer for the purpose of diagnosis. Wavelet transforms present one such approach for the purpose of compression. The same has been explored in paper with respect to wide variety of medical images. In this approach, the redundancy of the medical image and DWT coefficients are reduced through thresholding and further through Huffman encoding. This paper presents a lossy image compression technique which works well over most of the medical images.

**Index Terms**— Biorthogonal, DWT, Haar, Medical image compression, symlets.

## I. INTRODUCTION

Traditional image compression techniques have been designed to exploit the statistical redundancy present within real world images. The discrete cosine transforms (DCT), DPCM, and the entropy coding of subband images are all examples of this statistical approach. Removing redundancy can only give a limited amount of compression; to achieve high ratios, some of the non-redundant information must also be removed. Wavelet transform provides one such approach for image compression. [1][2]. Medical image compression is a challenge as the high frequency components may contain details relevant for medical diagnosis. In medical image compression applications, diagnosis is effective only when compression techniques preserve all the relevant and important image information needed. Thus, most of applications such as telemedicine and fast searching and browsing of medical volumetric data suffer from this limitation. For these kinds of applications, lossy compression seems to be an appropriate alternative. DICOM permits lossy image compression by a JPEG baseline system for ultrasonic echo images but suffers due to their inherent poor resolution [3]. Important properties of wavelet transforms such as multiresolution representation, energy compaction, blocking artifacts and decorrelation, has made the discrete wavelet transform (DWT) one of the most important techniques for image and video compression in the last decade and it has been adopted by JPEG 2000 standard [4]. In

Fact there is no single wavelet, which will always provide the best performance. Since there are many wavelet filters available, each with the different set of basic functions, the choice of wavelet filters is very vital factor to gain a good coding performance [5]. Therefore, one of the intent of this paper is also to investigate the effect of applying different types of wavelet for lossy compression of medical images.

## II. CODING SYSTEM FOR MEDICAL IMAGES

The images can be transferred from one domain to another. Applying wavelet transforms over the images converts them from spatial domain to time-scale domain. For the purpose of compression a basic system is presented and later the technique of transformation is discussed.

### A. Basic Model of Compression System

Most of the compression systems are based upon reducing the redundant information present in the signal whether it is 1D signal or 2D signal like image. Sometime redundancy reduction process is performed over the transformed signal rather than the original signal itself. The redundancy depends upon the entropy of the signal. Fig. 1 shows the basic model of the compression system based on redundancy in data. [6]

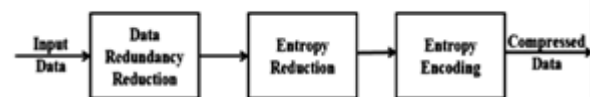


Fig 1 –Basic Model of Compression system

Redundancy reduction removes highly correlated data which is more in case of image due to much of the low frequency content in it. Discrete Wavelet Transform (DWT) has emerged as a popular technique for redundancy reduction. DWT has high decorrelation and energy compaction efficiency. Nonsignificant information is removed from the data by this process but it is a non reversible process electronically for review.

The popular entropy coding techniques are Huffman coding and Arithmetic coding which are used many times in compressing data and also in image compression techniques.

### B. Wavelet Transforms

One-dimensional wavelet theory defines a function  $\Psi$ , the wavelet, and its associated scaling function  $\Phi$ , such that the family of functions  $\{\Psi^j(x)\}_{j \in \mathbb{Z}}$ , where  $\Psi^j(x) = \sqrt{2^j} \Psi(2^j(x))$ , are orthonormal.

The continuous wavelet transform is defined by eq. 1.

**Manuscript received on April 26, 2012.**

**Ruchika**, Department of Electrical & Instrumentation Engineering, Thapar University, Patiala, Punjab, India, Mobile No.-91-9888679922, (e-mail: ruchika.mehta@thapar.edu).

**Mooninder Singh**, Department of Electrical & Instrumentation Engineering, Thapar University, Patiala, Punjab, India, Mobile No.-91-9855051314, (e-mail: mooninder@gmail.com).

**Anant Raj Singh**, Department of Electrical & Instrumentation Engineering, Thapar University, Patiala, Punjab, India, Mobile No.-91-9592719515, (e-mail: anantrajasingh@gmail.com).

$$C(a, b; f(t), \Psi(t)) = \int_{-\infty}^{\infty} f(t) \frac{1}{\sqrt{a}} \Psi^* \left( \frac{t-b}{a} \right) dt \dots (1)$$

Where,  $a$  is the Scaling Function,  $b$  is Shifting Function and  $\Psi(t)$  is the Wavelet function. [7]

For the formulation of Discrete Wavelet Transform, the scale and shift parameters are discretized as,

$$\begin{aligned} a &= a_0^m, \text{ and} \\ b &= n b_0 \end{aligned}$$

Thus the Analyzing Wavelet is also discretized as follows:

$$\Psi_{m,n}(t) = a_0^{-m/2} \Psi \left( \frac{t-nb_0}{a_0^m} \right) \dots (2)$$

Where,  $m$  and  $n$  are integer values.

Thus discrete wavelet transform and its inverse transform are defined as follows:

$$\begin{aligned} S_{m,n} &= \int_{-\infty}^{\infty} \Psi_{m,n}'(t) s(t) dt \\ s(t) &= k_{\Psi} \sum_m \sum_n S_{m,n} \Psi_{m,n}(t) \end{aligned} \dots (3)$$

Where,  $k_{\Psi}$  is a constant value for normalization.

The function  $\Psi_{m,n}(t)$  provides sampling points on the scale-time plane; these are linear sampling points in the time (b-axis) direction but logarithmic in the scale (a-axis) direction.

The most common situation is when  $a_0$  is chosen as  $a_0 = 2^{1/v}$ . Where  $v$  is an integer value; and those  $v$  pieces of  $\Psi_{m,n}(t)$  are processed together as one group.

For images, we use the hierarchical wavelet decomposition suggested by Mallat [8]. The high pass filters,  $H$  and the low pass filters,  $L$  are applied to the image in both the horizontal and vertical directions i.e. over rows and columns of the image matrix. The filtered outputs are subsampled signals, each by a factor of two, generating selective high-pass subbands details oriented in three directions viz. horizontal, diagonal and vertical; LH, HH and HL respectively. And also a low-pass approximation subband, LL obtained by applying low pass filter in horizontal and vertical direction. Fig. 2(a) shows wavelet subband decomposition of an image. The process is then repeated over the LL band, approximation, to generate the next level of the decomposition subband. Fig. 2(b) illustrates this wavelet image decomposition for any arbitrary  $j$ th level subband. Thus three octaves of decomposition will lead to ten decomposed subbands. Fig. 3(a) and 3(b) shows a typical MRI image decomposed in this way, up to first and third octave of decomposition respectively.

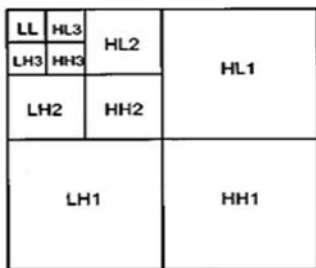


Fig. 2(a)

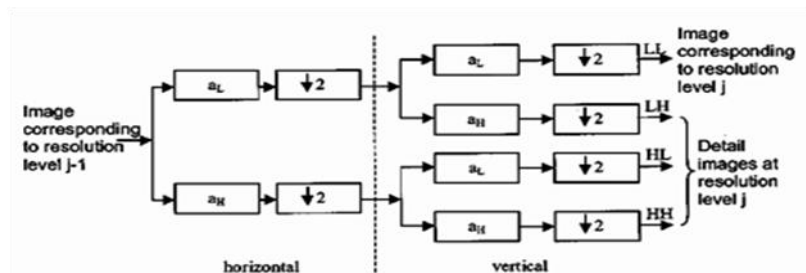


Fig. 2(b)

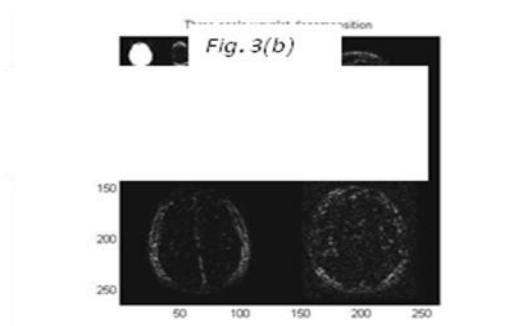
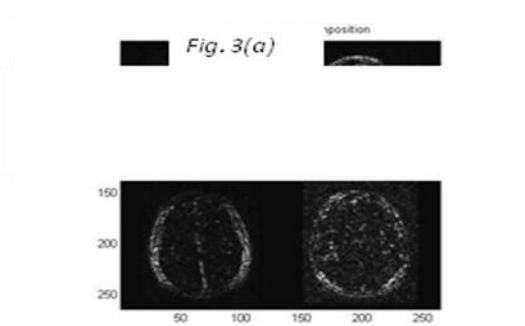


Fig. 2 – (a) Wavelet Subband Decomposition of image, (b) Decomposition of image to  $j^{th}$  level.

Fig. 3 – (a) Wavelet Decomposition of MRI brain image upto first level, (b) Wavelet Decomposition upto third level

**Huffman Encoding**

As Huffman codes belong to a family of codes which are variable in codeword length, which means that individual symbols which makes a message are represented (encoded) with bit sequences that have distinct length [9].

This helps to decrease the amount of redundancy in message data. Decreasing the redundancy in data by Huffman codes is based on the fact that distinct symbols have distinct probabilities of incidence. This helps to create code words, which really contribute to redundancy. Symbols with higher probabilities of incidence are coded with shorter code words, while symbols with higher probabilities are coded with longer code words.

**A. Thresholding**

The images are initially transformed by wavelet transform at one level. Then the threshold value, Thr, based on the transform coefficients is defined by eq. 4.

$$\text{Thr} = C(r \times n) \quad \dots (4)$$

$$C_{\text{New}} = \{C_i \mid \forall i \langle \text{Thr}, C(i) = 0 \rangle\} \quad \dots (5)$$

Where, n is the number of detail coefficients, C is the wavelet coefficient vector and r is the remaining rate in percent. Then the renewed wavelet coefficients  $C_{\text{New}}$  is as described in eq. 5.

**III. ALGORITHM FOR COMPRESSION**

The compression algorithm for medical image compression based on the wavelet transforms is given in following steps.

For Compressing the Medical Image:

1. The DWT of the medical image is generated by obtaining wavelet decomposition coefficients for the desired levels. The numbers of levels are decided by the entropy of the image.
2. A threshold for the decomposed image coefficients is selected, below which all the coefficients are made zero. This reduces the band space of the image signal, as large number of coefficients are made zero.
3. Huffman encoding on the thresholded coefficients is applied to reduce the redundancy in the coefficient data.
4. The thresholded and Huffman encoded coefficients are saved instead of the image.

For Uncompressing the Medical Image:

1. When the image is to be uncompressed, the Huffman decoding is done on the coefficients and the threshold coefficients are obtained.
2. Image is regenerated from these threshold coefficients by taking inverse discrete wavelet transform (IDWT).

**IV. RESULTS**

Results have been obtained by calculating few parameters obtained by the comparing original image and uncompressed image. They are defined as follows:

**(i) Mean Square Error (MSE):** It is the cumulative squared error between original and recovered image. It is defined by eq. 6.

$$MSE = \frac{1}{mn} \sum_{i=0}^{m-1} \sum_{j=0}^{n-1} ||I(i,j) - K(i,j)||^2 \quad \dots (6)$$

Where, I is the original image and K is the uncompressed image. The dimension of the images is m x n.

Thus MSE should be as low as possible for effective compression.

**(ii) Peak Signal to Noise Ratio (PSNR):** It is most commonly used as a measure of quality of reconstruction of lossy compression. It is the ratio between the maximum possible power of a signal and the power of corrupting noise that affects the fidelity of its representation; defined by eq. 7.

$$PSNR = 20 \log_{10} \left( \frac{MAX_i}{\sqrt{MSE}} \right) \quad \dots (7)$$

Where,  $MAX_i$  is the maximum possible pixel value of the image. PSNR should be as high as possible.

**(iii) Bit Per Pixel (BPP):** It is number of bits used to encode each pixel value. Thus for the purpose of compression BPP should be less to reduce storage on the memory.

**(iv) Compression Ratio (CR):** It is defined as the rate of the size of the original image data over the size of the compressed image data.

$$C_R = \frac{n_1}{n_2} \quad \dots (8)$$

where  $C_R$  is the compression ratio,  $n_1$  and  $n_2$  is the number of information carrying units in the original and encoded images respectively. CR is express in percentage.

The results over the images have been obtained using Haar, Biothogonal 4.4 and Symlet 8 wavelets. Results are analyzed in tabular form, images and graphs. The Image results are shown in Appendix.

The First test image is that of a MRI of a human skull. The best result was obtained with Biorthogonal 4.4 wavelet. The MSE is as low as 20.47 and PSNR is 35.01dB at the BPP of 0.977. The compression ratio at this point is 12.21%. The image is illustrated in Fig. 7(a), in the Appendix. The results of various parameters of the Skull MRI image are recorded in Table-I over different wavelets.

**Table –I: Values of MRI skull Image Parameters.**

Image	Wave let Used	BPP	MSE	PSNR (dB)	CR %
MRI Skull	Haar	1.088 5	23.3135	34.454	13.606
		2.305 7	67.0454	29.867	28.822
	Bior 4.4	0.977 4	20.4707	35.019	12.217
		2.151 4	80.4739	29.074	26.893
	Sym8	1.002 5	21.8439	34.737	12.532
		2.142 3	85.2065	28.826	26.779

A graph between PSNR and BPP is plotted for various

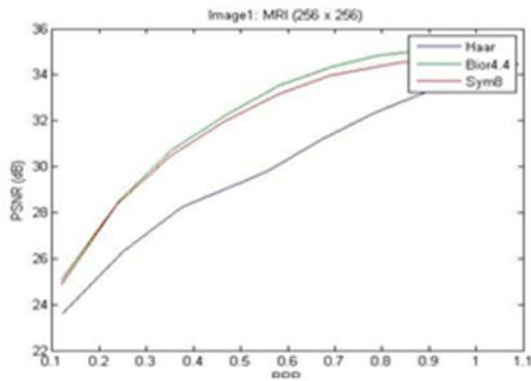


**Fig. 4- PSNR v/s BPP plot of MRI image for various wavelets**

wavelets applied over the image. Fig. 4 shows the plot of PSNR v/s BPP for the MRI Skull image. The results obtained with Symlet8 are little less than Bior4.4. Symlet8 and Bior 4.4 have similar characteristic curves of PSNR v/s BPP. The Symlet8 curve remains a little below than that of Bior4.4.

In the second test Image that of Cardiac MR of Vertical Left outflow tract of heart, the best results are obtained with Biorthogonal4.4 at BPP of 0.9903 with resulting MSE of 28.9482dB. The result has been enlisted in Table-II, which shows the values of various parameters at different point for the image. The similar characteristic curve of PSNR v/s BPP are plotted for the Cardiac image and are shown in fig. 5. The characteristic curve of Symlet8 is just below the Bior4.4 curve and also touches it at a point but never crosses it. The Haar Curve is very similar to the Biorthogonal4.4 curve in shape but is much below than the Biorthogonal4.4 curve. Hence, it offers much less PSNR at a particular BPP than the Biorthogonal4.4 and Symlet 8, for this particular image.

**Table –II: Values of Cardiac MR Image Parameters.**

Image	Wavelet Used	BPP	MSE	PSNR (dB)	CR %
Cardiac MR	Haar	1.0773	40.7957	32.024	13.467
		2.3215	89.9439	28.591	29.019
	Bior 4.4	0.9903	28.9482	33.514	12.379
		2.1997	112.046	27.636	27.496
	Sym8	0.9653	32.5184	33.009	12.066
		2.1748	116.124	27.481	27.185

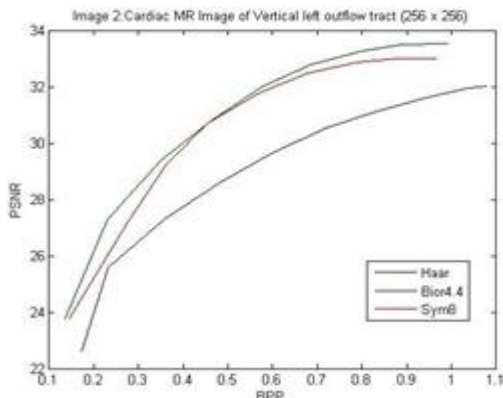


**Fig. 5- PSNR v/s BPP plot of MR image for various wavelets**

On the third Image, that of Ultrasound of Liver Cyst the best results are obtained with Haar wavelet. Biorthogonal4.4 and Symlet 8 showed a poorer result. The results are recorded in tabular form in Table-III for the image. The curves for PSNR v/s BPP are plotted for various values and are shown in Fig. 6. All the characteristic curves of all the wavelets were clustered around almost the same region. Symlet8 and Biorthogonal Curves meet in the end. Haar Curve crosses the two and comes ahead in terms of PSNR at the same BPP levels.

**Table –III: Values of Ultrasound Image Parameters.**

Image	Wavelet Used	BPP	MSE	PSNR (dB)	CR %
Ultra Sound	Haar	0.8293	42.6176	31.834	10.366
		1.8457	212.012	24.867	23.071
	Bior 4.4	0.7326	48.8650	31.240	9.1577
		1.9873	324.245	23.022	24.842
	Sym8	0.8264	48.6307	31.261	10.330
		1.9887	263.204	23.927	24.859

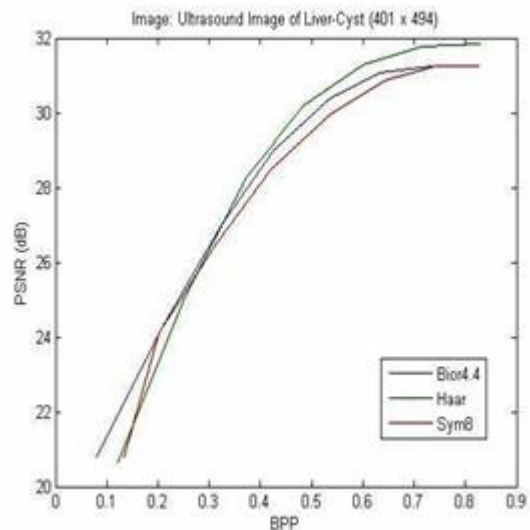


**Fig. 6- PSNR v/s BPP plot of Liver Ultrasound image for various wavelets**

**V. CONCLUSION**

The algorithm works well over the images as shown by the results. Huffman encoding is a lossless data compression technique. At the most optimal compression the original and uncompressed from wavelet coefficient is almost the very same. Future scope depends on developing a trained system which can automatically detect type of medical image and determine which suit able wavelet will produce the best compression on it. One such system could be developed using Neural Networks trained on specific images by different wavelets.

APPENDIX – IMAGE RESULTS

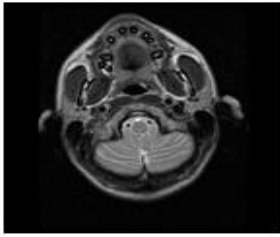


Fig. 7(a)



Fig. 7(b)



Fig. 7(c)

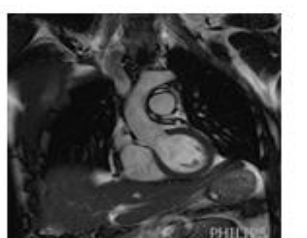


Fig. 8(a)

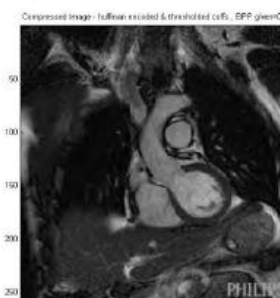


Fig. 8(b)



Fig. 8(c)



Fig. 9(a)



Fig. 9(b)

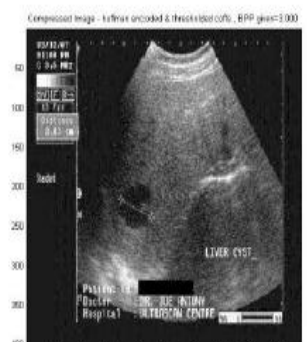


Fig. 9(c)

Fig. 7 – (a) Original MRI Skull Image,  
(b) CR%=12.217, BPP=0.9774, PSNR=35.019,  
(c) CR%=26.893, BPP=2.1514, PSNR=29.074

Fig. 8 – (a) Original MR Cardiac Tract Image,  
(b) CR%=12.379, BPP=0.9903, PSNR=33.514,  
(c) CR%=27.496, BPP=2.19974, PSNR=27.636

Fig. 9 – (a) Original Ultrasound Liver Cyst Image,  
(b) CR%=10.366, BPP=0.8293, PSNR=31.834,  
(c) CR%=23.071, BPP=1.8457, PSNR=24.867

REFERENCES

1. M. Antonini, et al.: "Image Coding Using Wavelet Transforms" *IEEE Trans. Image Processing*, vol. 1, no. 2, pp. 205-220, April 1992.
2. Amir Averbuch, et al.: "Image Compression Using Wavelet Transform and Multiresolution Decomposition", *IEEE Trans. Image Processing*; vol. 5, no. 1, pp 4-15, January 1996.
3. N. Sahba, et al.: "An Optimized Two-Stage Method for Ultrasound Breast Image Compression," *4th Kuala Lumpur International Conf. Biomedical Engg.*, vol. 21, June 2008, pp. 515-518.
4. M.D.Adams and R.Ward; "Wavelet Transforms in JPEG 2000 Standard", *IEEE Pacific Rem Conf. on Comm. Comp. & Signal Pross.*, 2001, vol. 1 pp. 160-163.
5. S. Udomhunsakul and K. Hamamoto, "Wavelet filters comparison for ultrasonic image compression," *Conf. IEEE TENCON*, vol. 1, Nov. 2004, pp. 171-174.
6. T. Acharya and P. Tsai, *JPEG2000 Standard for Image Compression: Concepts, Algorithms and VLSI Architectures*, John Wiley & Sons, 2005, pp. 24-30.
7. I. Daubechies; "Ten Lectures on Wavelet".
8. S. Mallat, "A theory for multiresolution signal decomposition: The wavelet representation," *IEEE Trans. Pat. Anal. Machine Intell.*, vol. 11, no. 7, July 1989, pp. 674-693.
9. D.A. Huffman, "A Method for the Construction of Minimum-Redundancy Codes", *Proceedings of the I.R.E.*, September 1952, pp. 1098-1102.

AUTHORS PROFILE



**Ruchika** is working as Lecturer in the Electrical and instrumentation Engineering Department at Thapar University, Patiala, Punjab, India. She received her graduate degree in Instrumentation and Control Engineering from Kurukshetra University, Kurukshetra, Haryana, India in 2005 and ME degree in Instrumentation Engineering from National Institute of Technical Teachers Training and Research, Chandigarh, India, in 2009. She received S P Luthra Gold Medal along with Academic award at Post Graduation level. She teaches undergraduate and postgraduate courses in Electrical and instrumentation engineering. Her major research interests are Image Processing, Microcontroller, and Bio medical Instrumentation.



**Mooninder Singh** is working is an Asst. Prof. in Department of Electrical and Instrumentation at Thapar University, Patiala, Punjab, India. He received his postgraduate degree of M.Tech from Punjab University, Chandigarh, India in Instrumentation in 2004. He received his B.Tech degree in 2002. He teaches both undergraduate and postgraduate Electrical and Instrumentation courses at Thapar University Patiala. His areas of research are Digital and Advanced Signal Processing and Microcontroller based signal processing. He also pursuing is Ph.D in the area of Bio-medical signal processing from the Department of Electrical and Instrument. Thapar University, Patiala, Punjab.



**Anant Raj Singh** is pursuing his postgraduate Degree of M.E. in Electronics Instrumentation and Control Engineering form the Department of Electrical and Instrumentation, Thapar University Patiala, Punjab, India. He received his graduate degree in 2010 in Electronics and Instrumentation from U.P. Technical University. His areas of research are wavelet based advanced signal processing, image processing. His areas of interest also include clustering and optimization techniques.

